Comparability of compressed sensing-based gradient echo perfusion sequence SPARSE and conventional gradient echo sequence in assessment of myocardial ischemia

Muehlberg, F.; Stoetzner, A.; Forman, C.; Schmidt, M.; Riazy, L.; Dieringer, M.; ... ; Schulz-Menger, J.

European Journal of Radiology 131 (2020) 109213

Contents lists available at ScienceDirect

European Journal of Radiology

journal homepage: www.elsevier.com/locate/ejrad

Research article

Comparability of compressed sensing-based gradient echo perfusion sequence SPARSE and conventional gradient echo sequence in assessment of myocardial ischemia

Fabian Muehlberg [a,*,1], Arthur Stoetzner [a,1], Christoph Forman [b], Michaela Schmidt [b], Leili Riazy [a,1], Matthias Dieringer [b], Rob van der Geest [c], Carsten Schwenke [d], Jeanette Schulz-Menger [a,1]

[a] HELIOS Hospital Berlin-Buch, Department of Cardiology and Nephrology, Lindenberger Weg 80, 13125 Berlin, Germany
[b] Siemens Healthineers, Diagnostic Imaging, Magnetic Resonance, Allee am Röthelheimpark 2, 91052 Erlangen, Germany
[c] Division of Image Processing, Department of Radiology, Leiden University Medical Center, Albinusdreef 2, 2333 ZA Leiden, the Netherlands
[d] SCO:SSiS Statistical Consulting, Karmeliterweg 42, 13465 Berlin, Germany

ARTICLE INFO

Keywords:
Perfusion
Compressed sensing
CMR
Stress MRI
Coronary artery disease
Non-invasive stress test

ABSTRACT

Purpose: Stress perfusion imaging plays a major role in non-invasive detection of coronary artery disease. We compared a compressed sensing-based and a conventional gradient echo perfusion sequence with regard to image quality and diagnostic performance.

Method: Patients sent for coronary angiography due to pathologic stress perfusion CMR were recruited. All patients underwent two adenosine stress CMR using conventional TurboFLASH and prototype SPARSE sequence as well as quantitative coronary angiography with fractional flow reserve (FFR) within 6 weeks. Coronary angiography was considered gold standard with FFR < 0.75 or visual stenosis >90 % for identification of myocardial ischemia. Diagnostic performance of perfusion imaging was assessed in basal, mid-ventricular and apical slices by quantification of myocardial perfusion reserve (MPR) analysis utilizing the signal upslope method and a deconvolution technique using the fermi function model.

Results: 23 patients with mean age of 69.6 ± 8.9 years were enrolled. 46 % were female.

Image quality was similar in conventional TurboFLASH sequence and SPARSE sequence (2.9 ± 0.5 vs 3.1 ± 0.7, p = 0,06). SPARSE sequence showed higher contrast-to-noise ratio (52.1 ± 27.4 vs 40.5 ± 17.6, $p < 0.01$) and signal-to-noise ratio (15.6 ± 6.2 vs 13.2 ± 4.2, $p < 0.01$) than TurboFLASH sequence. Dark-rim artifacts occurred less often with SPARSE (9 % of segments) than with TurboFLASH (23 %).

In visual assessment of perfusion defects, SPARSE sequence detected less false-positive perfusion defects (n = 1) than TurboFLASH sequence (n = 3).

Quantitative perfusion analysis on segment basis showed equal detection of perfusion defects for TurboFLASH and SPARSE with both upslope MPR analysis (TurboFLASH 0.88 ± 0.18; SPARSE 0.77 ± 0.26; p = 0.06) and fermi function model (TurboFLASH 0.85 ± 0.24; SPARSE 0.76 ± 0.30; p = 0.13).

Abbreviations: 2D, two-dimensional; 3D, three-dimensional; AHA, American Heart Association; BMI, body mass index; CAD, coronary artery disease; CMR, cardiovascular magnetic resonance; CNR, contrast-to-noise ratio; CS, compressed sensing; DRA, dark rim artifact; FISTA, Fast Iterative Shrinkage-Thresholding Algorithm; FLASH, fast low angle shot; FOV, field of view; FFR, fractional flow reserve; LGE, late gadolinium enhancement; LV, left ventricular; LV-EDV, left ventricular enddiastolic volume; LV-EF, left ventricular ejection fraction; LV-M, left ventricular mass; MBF, myocardial blow flow; MPR, myocardial perfusion reserve; MR, magnetic resonance; MRI, Magnetic resonance imaging; ROI, region of interest; SD, standard deviation; SNR, signal-to-noise ratio; SPECT, single photon emission computed tomography; SSFP, steady-state free precession; TE, echo time.

* Corresponding author.
E-mail addresses: fabian.muehlberg@helios-gesundheit.de (F. Muehlberg), arthurstoetzner@gmail.com (A. Stoetzner), christoph.forman@siemens-healthineers.com (C. Forman), michaela.schmidt@siemens-healthineers.com (M. Schmidt), lei-r@hotmail.de (L. Riazy), matthias.dieringer@siemens-healthineers.com (M. Dieringer), R.J.van_der_Geest@lumc.nl (R. der Geest), carsten.schwenke@scossis.de (C. Schwenke), jeanette.schulz-menger@charite.de (J. Schulz-Menger).
[1] Working Group on Cardiovascular Magnetic Resonance, Experimental and Clinical Research Center - a joint cooperation between the Charité Medical Faculty and the Max-Delbrück Center for Molecular Medicine.

https://doi.org/10.1016/j.ejrad.2020.109213
Received 31 March 2020; Received in revised form 8 July 2020; Accepted 3 August 2020
Available online 11 August 2020

Conclusions: Compressed sensing perfusion imaging using SPARSE sequence allows reliable detection of myocardial ischemia.

1. Introduction

Contrast-enhanced first-pass myocardial perfusion magnetic resonance (MR) is an established non-invasive method for detection of coronary artery disease and holds prognostic value [1,2]. In analogy to other MR techniques, conventional myocardial perfusion sequences have restricted spatial in-plane resolution and limited myocardial coverage as they typically cover three short-axis planes of the left ventricular myocardium [3]. The limiting factor for these constraints is the length of the cardiac cycle, which leads to a short time window for image acquisition during systole.

For this reason, conventional imaging methods compromise in spatio-temporal resolution. While the diagnostic accuracy of stress perfusion MRI has been shown to be equivalent or superior to alternative non-invasive imaging techniques such as SPECT (single photon emission computed tomography) [4], an enhanced spatio-temporal resolution may increase detection rates of smaller regions of ischemia and, thereby, further strengthen the role of cardiac MRI in diagnostic of relevant coronary artery disease (CAD).

In myocardial first-pass perfusion, the total acquisition time is determined by the contrast enhancement and the visualization of its tissue perfusion dynamics. Hence, the speed-up of the highly accelerated methods is typically utilized to improve the spatial resolution, which promises to reduce the effects of the sub-endocardial dark-rim artefact [5]. Parallel imaging is the established acceleration technique to shorten the scan time in clinical routine. However, with higher acceleration factors parallel imaging techniques regularly face reductions of signal-to-noise ratio (SNR) [6]. To overcome this limitation, k-t spatio-temporal models [6] and compressed sensing methods [7] have been proposed for accelerated data acquisition. The spatio-temporal redundancy in subsequent frames is typically exploited to recover the signal of the sub-sampled data in the compressed sensing reconstruction. This has been successfully demonstrated when the inter-frame motion is minimal, e.g. for cardiac cine imaging. However, for perfusion imaging the presence of respiration or irregular heartbeats leads to an increased anatomical misalignment and, at the same time, reduces the spatio-temporal redundancy. As a consequence, the resulting images may suffer from temporal blurring or residual motion artefacts that impact the diagnostic value of the images. Dense non-rigid motion models were introduced in the compressed sensing reconstruction to address this limitation [8–11].

In this study, we prospectively compared a highly accelerated sequence featuring prospective incoherent sub-sampling (SPARSE) with a conventional clinical protocol (TurboFLASH) in myocardial first-pass perfusion and in patients with known or suspected coronary artery disease. In contrast to previous work, the motion model is calculated only once and neighboring frames of intermediate reconstructed images were registered with a diffeomorphic image registration [11,12]. Image quality was qualitatively and quantitatively assessed analyzing the contrast dynamics of cardiac perfusion and the diagnostic outcome was compared to assessment by fractional flow reserve (FFR) in coronary angiography as reference standard. We hypothesized that SPARSE perfusion sequence would be comparable to TurboFLASH sequence with regard to identifying area of myocardial ischemia.

2. Materials and methods

2.1. Study population

The Charité University Medicine ethics board at Charité Campus Mitte, Berlin, Germany, approved the present prospective single-center study. Reference number: EA1/081/15. Patients were enrolled consecutively upon written informed consent. All patients were scheduled for coronary angiography due to known or suspected CAD following a routine adenosine-stress perfusion MR. Exclusion criteria were chronic renal failure with glomerular filtration rate <30 mL/min/1.73m^2, arrhythmia, any cardiac MR or adenosine contraindication or known adverse reaction from gadolinium-based contrast media. All patients were instructed to refrain from caffeine-containing substances 24 h before each examination.

2.2. MR data acquisition

Patients received two separate MR scans prior to coronary angiography. All MR exams were conducted using a 1.5T MR system (MAGNETOM AvantoFit, Siemens Healthineers®, Erlangen, Germany). Cardiac synchronization was ensured using a vector ECG. An 18-element coil array in combination with a 32-element spine array was used for signal reception. In each MR exam, standard steady state free precession (SSFP) cine sequences were acquired in left ventricular (LV) long-axis to assess myocardial anatomy and function. Myocardial perfusion imaging was planned in three short axis planes covering the basal, mid-ventricular and apical LV myocardium without overlap and special emphasis on excluding the LV outflow tract in the basal plane. A native test perfusion sequence with duration of five heart cycles was performed to assess artifacts and to correct slice positioning. Upon approval of the test sequence by an MR experienced physician, adenosine was administered intravenously at a dose of 140 µg/kg/min. The heart rate was continuously monitored until the onset of adenosine-induced symptoms and increase of heart rate occurred. Stress perfusion imaging was performed under free-breathing after intravenous bolus application of 0.1 mmol/kg body weight of gadoteridol (Prohance®, Bracco, Milan, Italy) followed by 20 ml saline flush. After a 10-min waiting period the identical perfusion sequence was repeated in the same fashion at rest. Perfusion data at stress and rest was acquired over 30 consecutive cardiac cycles and was performed in free breathing. Details on each perfusion sequence used are described in the next paragraph.

Following another 10-min waiting period, late gadolinium enhancement imaging was performed using a standard 2D phase-sensitive inversion recovery sequence (TE: 5.17 ms, flip angle: 30°, FOV: 400 mm, matrix: 192 × 256 mm, slice thickness: 7 mm without gap) in short-axis geometry. Inversion recovery pre-pulse delay was determined using a Look-Locker sequence.

2.3. Perfusion sequence parameters

In the first MR exam, a conventional, motion-corrected 2D TurboFLASH perfusion sequence was used for perfusion imaging while we used a prototype 2D gradient echo sequence featuring incoherent sampling and compressed sensing imaging reconstruction (SPARSE) in the second exam. Most of the imaging parameters of both sequences were matched as shown in Table 1. The increased acceleration of 4.2 in the prototype sequence was utilized to improve the spatial in-plane resolution from 1.9 mm^2 to 1.6 mm^2. Similar to the highly accelerated cine acquisition using compressed sensing, the data acquisition of the prototype sequence is sped up using an incoherent phase encoding sampling pattern along the time axis (Fig. 1). After data acquisition, the coil sensitivity maps are calculated from the fully sampled region in k-space center after temporal averaging of the data from all time frames. Compressed sensing image reconstruction was performed using the FISTA

Table 1
Perfusion sequence parameters. TR = repetition time; TE = echo time; TI = inversion time; FOV = field of view.

Parameter	Unit	TurboFLASH	SPARSE
Slice thickness	[mm]	8	8
TR	[ms]	180	162
TE	[ms]	1.18	1.18
TI	[ms]	110	105
Bandwidth	[Hz]	650	650
Flip angle		12°	15°
Matrix	[mm]	192 × 152	256 × 194
FOV	[mm]	380 × 300	400 × 318
Pixel size	[mm]	1.92 × 1.92	1.64 × 1.64

algorithm and using the following minimization scheme:

$$\mathbf{m} = \min_{\hat{\mathbf{m}}} \|\mathbf{E}\hat{\mathbf{m}} - \mathbf{s}\|_2^2 + \lambda \|\mathbf{W}\mathbf{T}\hat{\mathbf{m}}\|_1 ,$$

where **E** is the MR system matrix consisting of the Fourier transform, the sampling pattern, and the coil sensitivity maps. The measured data is denoted by **s**, **m** is the reconstructed image, **W** is a wavelet transform, and λ is the regularization parameter. The non-rigid deformations of the dense motion model are described in **T** implementing bilinear interpolation. At the beginning of the iterative optimization, **T** is initialized as identity transform, which means that it is turned off. After 20 iterations, the intermediate reconstructed images are utilized as input for a diffeomorphic image registration [6] to calculate the non-rigid deformation fields. In contrast to [5], the motion model is calculated only once. (Supplementary Fig. 2) The dense motion model **T** is updated based on the computed deformation fields. Subsequently, the motion model is used to improve the spatio-temporal redundancy during the regularization step of the compressed sensing reconstruction. In total, the optimization was run for 40 iterations and with $\lambda = 2{\cdot}10^{-2}$ of the maximum intensity. A preliminary study on a subset of the patient data (n = 5) was performed with and without usage of the motion model. This preliminary study showed an improved image quality and a better visualization of the contrast agent dynamics both qualitatively and quantitatively, when the motion model was applied in the image reconstruction. As illustrated in Fig. 2 the reduced misalignment also reduced the temporal blurring in the images, which allowed a better depiction of a perfusion deficit. Hence, only the method using the motion model was applied for image reconstruction of acquired data from the prototype sequence in the current study.

2.4. Coronary angiography and fractional flow reserve (FFR) assessment

Coronary angiography was performed by an experienced interventional cardiologist using routine techniques. Every major coronary vessel was acquired in at least two orthogonal views. FFR measurements were conducted in every coronary vessel >2 mm in diameter that had visual stenosis >50 % and <90 %. Smaller vessels were considered non-significant in accordance to established guidelines. FFR was assessed using a 0.014-inch coronary pressure wire. FFR values <0.75 were considered hemodynamically significant. Subtotally occluded coronary vessels (visual stenosis >90 %) were considered hemodynamically relevant without FFR assessment. Coronary angiography was defined as reference standard for detection of relevant myocardial perfusion deficits in this study. All stenoses were assigned to the appropriate segment of a modified AHA 16-segment model according to coronary dominance as published before [1].

2.5. Qualitative image and perfusion analysis

MR images were visually analyzed by three blinded MR experienced readers (SCMR Level III) using the post-processing software CVI42®, release 5.6.2 (Circle Cardiovascular Imaging Inc., Calgary, Canada). General image quality was graded separately for stress and rest perfusion sequences on a scale between 0 and 4 (0 = non-diagnostic, 1=poor, 2=moderate, 3= good, 4=excellent). Basal, mid-ventricular and apical perfusion plane were segmented into 16 segments according to the 17-segments-AHA (American Heart Association) model excluding the furthest apical segment. Each segment was evaluated visually for presence of dark-rim artifacts and breathing artifacts for both readings.

Visual perfusion assessment was performed for each AHA segment in order to detect perfusion defects. This was done following published method [7]: any perfusion defect with >25 % transmurality persisting for >3 consecutive cardiac cycles that was not present at rest perfusion and not showing myocardial scar on LGE imaging, was marked as pathological.

2.6. Semi-quantitative image and perfusion analyses

Using the post-processing software CMR42®, morphologic and functional LV parameters LV end-diastolic volume (LV-EDV), LV ejection fraction (LV-EF) and LV mass (LV-M) were assessed on SSFP-cine long axis views (two- and four-chamber view).

Signal-to-noise ratio before contrast application (SNRpre) and at myocardial contrast peak (SNRpeak) and contrast-to-noise ratio (CNR) was assessed as previously described [8].

For semi-quantitative analysis of the perfusion datasets, two different methods were used. A signal intensity upslope-based model to estimate a myocardial perfusion reserve (MPR) as previously described by Nagel et al. [9] Secondly, we used a Fermi function constrained deconvolution model to quantify MPR. Post-processing was done on an adapted version of the Mass® Research Software (Version 2016-EXP, Leiden University Medical Center, Leiden, The Netherlands) to assess the myocardial blood flow (MBF). The MPR values were calculated as the ratio of MBF under adenosine stress divided by MBF at rest as previously established [10]. Semi-quantitative MPR values of remote myocardium were normalized for improved comparison between patients.

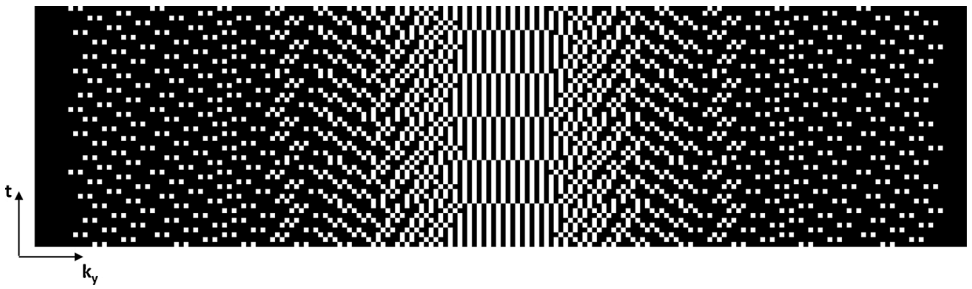

Fig. 1. Incoherent sampling pattern in the Cartesian phase-encoding direction (ky). The pattern is varied in the temporal dimension (t). The readout direction is fully sampled so that each dot represents a fully sampled line in the kx direction.

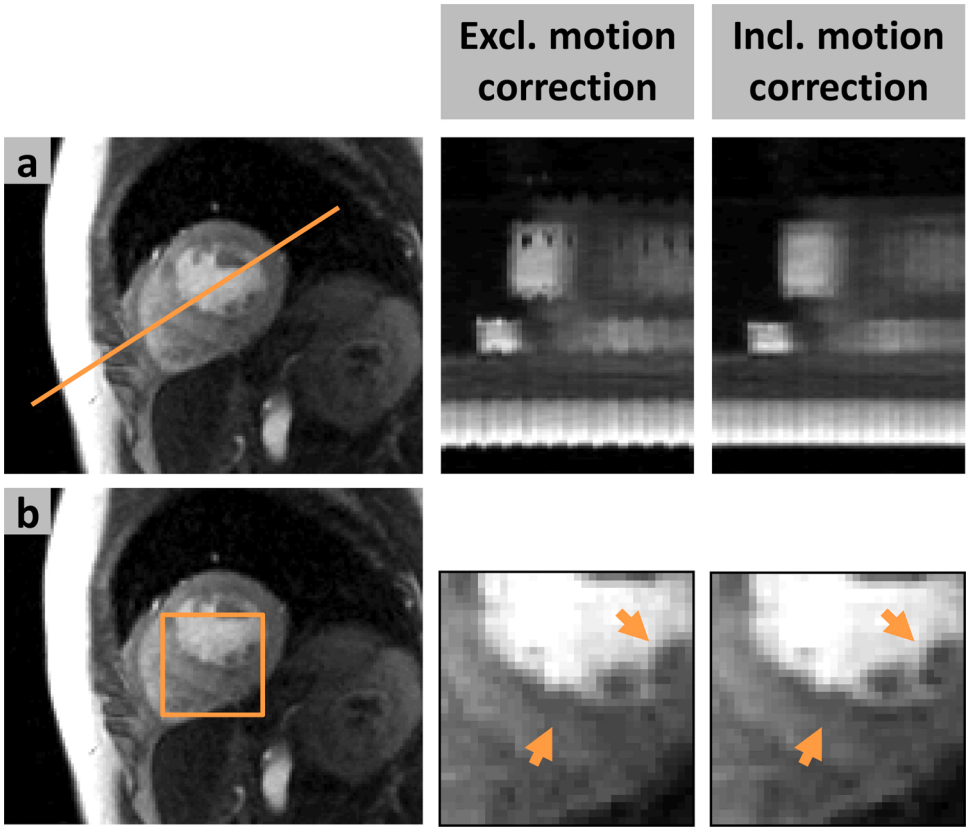

Fig. 2. Motion correction model. Exemplary images showing a) reduced voxel misalignment with motion correction resulting in b) better depiction of perfusion deficit.

2.7. Statistical analysis

Statistical analysis was performed using SPSS 17.0 (SPSS, Chicago, Illinois, USA). Data are expressed as means ± standard deviation (SD). Differences between the two sequences were compared using paired *t*-tests. Image quality and artifacts analysis were assessed using Wilcoxon signed ranks test. Mean values for SNR and CNR were compared using paired *t*-test and semi-quantitative perfusion analysis using least squares regression analysis. The visual assessment was directly compared to the results in coronary angiography. Interobserver variability was assessed using intraclass correlation coefficient calculations. Statistical significance was defined as $p < 0.05$.

3. Results

3.1. Study population

We initially consecutively recruited 26 patients, three patients needed to be excluded from analysis due to arrhythmia (n = 1) and incomplete data sets (n = 2). 23 patients completed all study exams successfully and where subject to all further analyses. Mean age of study participants was 69.6 ± 8.9 years, 46 % were female and 50 % had known CAD. Detailed patient characteristics are listed in Table 2A.

For further patient characterization and to assess comparability between both MR scans, left ventricular anatomy and function were assessed at both time points and revealed no significant difference for LV-EF (57.8 ± 8.1 % vs. 58.2 ± 7.8 %), LV-EDV (149.2 ± 25.4 mL vs. 145.1 ± 34.8 mL) or LV-Mass (81.0 ± 20.8 g vs. 82.0 ± 19.0 g). Heart rate, blood pressure and cardiac output were not different between both exams as well (see Table 2B). Mean time between both MR scans was 28 ± 28 days, while mean time between last MR scan and coronary angiography was 1 ± 3 days.

Table 2
A) Patient characteristics; B) Morphologic left ventricular parameters and hemodynamics at both MR scans. BMI = body mass index; CAD = coronary artery disease; PCI = percutaneous coronary intervention; CABG = coronary artery bypass graft: LVEF = left ventricular ejection fraction; LVEDV = left ventricular end-diastolic volume; LVM = left ventricular mass.

Parameter	Unit	Value
Age	[Years]	69.6 ± 8.9
Sex	[abs. male/female]	14/12
BMI	[kg/m^2]	28.3 ± 4.7
Known CAD	[abs. / %]	13 / 50 %
Previous PCI	[abs. / %]	11 / 42 %
Previous CABG	[abs. / %]	6 / 23 %
Excluded patients	[abs. / %]	3 / 11 %

Parameter	Unit	MR 1 (TurboFLASH)	MR 2 (SPARSE)	p value
LVEF	[%]	57.8 ± 8.1	58.2 ± 7.8	0.98
LVEDV	[ml]	149.2 ± 36.4	145.1 ± 34.8	0.13
LVM	[g]	81 ± 20.8	82.0 ± 19.0	0.28
Heart rate (rest)	[min^{-1}]	68 ± 12.0	67 ± 10.0	0.68
Heart rate (stress)	[min^{-1}]	86 ± 11.0	85 ± 14.0	0.28
Cardiac Output	[l/min]	5.8 ± 1.3	5.6 ± 1.5	0.09

3.2. Image quality

Subjective image quality score did not significantly differ between TurboFLASH (2.9 ± 0.5) and SPARSE (3.1 ± 0.6; p = 0.06). Image quality was good or excellent in 82 % of patients with TurboFLASH and in 85 % with SPARSE. No perfusion data was rated as bad or non-diagnostic in either SPARSE or TurboFLASH.

Dark rim (DRA) and breathing artefacts were detectable on both sequences. However, while TurboFLASH had DRA in 23 % of all investigated segments, SPARSE only showed DRA in 9 % of the segments.

DRA were mostly present in basal segments. (See supplementary Fig. 1 and supplementary video files as illustrative examples)

On TurboFLASH perfusion data, 26.8 % of patients had detectable breathing artefacts, while these were detected in only 7.7 % of SPARSE perfusion acquisitions.

CNR, SNR before contrast administration (SNRpre) and SNR at contrast peak (SNRpeak) were significantly higher with the SPARSE sequence (Table 3).

3.3. Qualitative (visual) perfusion analysis

Illustrative examples for perfusion defects with TurboFLASH and SPARSE sequence are shown in Fig. 3 (additional video files available in supplementary data). At patient level, coronary angiography revealed hemodynamically relevant coronary stenosis (FFR < 0.75) in 19 patients (73.1 %). All 19 patients also had visually detectable coherent perfusion defects in both TurboFLASH and SPARSE sequence. However, on TurboFLASH an additional three patients (11.5 %) had visual detection of perfusion defects while x-ray angiography as reference standard revealed FFR > 0.75 for all coronary vessels. Using SPARSE sequence, only one patient (3.8 %) had false-positive detection of perfusion defects (Table 4).

Small ischemia (<4/32 segments) was detected in two individuals, however, both still had relevant coronary stenosis upon FFR measurements. Moderate ischemia (4-8/32 segments) was detected in 16 patients with TurboFLASH and 15 individuals with SPARSE. Severe ischemia (>8/32 segments) was found in five patients with TurboFLASH and six patients on SPARSE.

At segment level, TurboFLASH had a visual perfusion defect sensitivity of 95 % with regards to angiography as standard of reference, for SPARSE sensitivity was 98 %. Specificity was 93 % for TurboFLASH and 97 % for SPARSE on the segment level.

3.4. Semi-quantitative perfusion analysis

Upslope-based and Fermi deconvolution-based analysis was performed in order to detect perfusion defects through mean MPR. As illustrated in Fig. 4, upslope-based analysis revealed similarly decreased MPR values in segments with ischemia on angiography for TurboFLASH (0.87 ± 0.18; CI = 0.85−0.90) and SPARSE sequence

(0.78 ± 0.26; CI = 0.73−0.83). With a p value of 0.06 there was no significant difference between both sequences.

Fermi deconvolution-based analysis showed similar results for ischemic perfusion segments with MPR values of (0.84 ± 0.24; CI = 0.81−0.88) for TurboFLASH and (0.76 ± 0.30; CI = 0.71−0.82) for SPARSE (see Fig. 4); p value for comparison of TurboFLASH and SPARSE was non-significant as well with p = 0.13. Interobserver variability was good with ICC of 0.83 (95 % confidence interval 0.75−0.89).

Table 3
Signal-to-noise and contrast-to-noise ratios.

Sequence	SNRpre	p	SNRpeak	p	CNR	p
TurboFLASH-Stress	13.21 ± 4.19	<0.001	53.74 ± 21.31	<0.001	40.52 ± 17.64	<0.001
SPARSE-Stress	15.58 ± 6.22		67.69 ± 32.11		52.12 ± 27.44	
TurboFLASH-Rest	20.7 ± 7.25	0.72	48.52 ± 16.48	0.23	27.82 ± 9.99	0.09
SPARSE-Rest	21.36 ± 8.23		51.63 ± 20.77		30.27 ± 13.32	

4. Discussion

In this study we compared an innovative, highly accelerated myocardial perfusion sequence featuring prospective incoherent subsampling (SPARSE) with a conventional Turbo-FLASH-based perfusion sequence in patients with known or suspected coronary artery disease and utilized FFR measurements in coronary angiography as reference standard. To the best of our knowledge, this is the first time this technique was applied in a reference standard-proven setting.

Major insights included: (1) there was no significant difference in overall image quality comparing both sequences, however, fewer dark rim and breathing artifacts as well as higher CNR and SNR using SPARSE were observed. (2) Upon visual perfusion analysis, all relevant coronary stenosis (FFR < 0.75) were detected in both sequences. However, with conventional Turbo-FLASH we detected more false-positive regions of ischemia than in SPARSE. (3) Quantitative perfusion image analysis showed no difference for both sequences in terms of mean MPR.

Compressed sensing (CS) techniques are promising acceleration tools for cardiovascular MRI in different types of sequences. They have been shown to accelerate self-gated cine images with acceleration factors of up to 15 [13], enabling image acquisition in as few as one cardiac cycle [14]. Early CS techniques have also been introduced for myocardial first-pass perfusion imaging and showed good feasibility in small numbers of animals and healthy volunteers [15,16]. Contrary, CS perfusion sequences have to our knowledge not been compared with a conventional Turbo-FLASH sequence and invasive FFR as gold standard.

In this study we found significantly fewer cases of dark rim artifacts using SPARSE than in Turbo-FLASH (7.7 % vs. 26.8 %). The scan acceleration provided by the CS acquisition enabled an improved spatial in-plane resolution from 1.9 to 1.6 mm. Previous studies showed a strong correlation between DRA and spatial resolution and that a high spatial resolution led to a reduction of these artefacts [17].

DRA represent a major diagnostic obstacle as they may lead to false-positive ischemia testing and thereby influence the diagnostic accuracy of the method [18]. This may have been also attributable to this study as there were three patients with false-positive ischemia testing using conventional TurboFLASH while only one patient was tested falsely positive using SPARSE.

Furthermore, less respiratory motion artifacts were observed in the images acquired with the SPARSE method. This result can be attributed to the integration of the motion-correction into the CS image reconstruction. Aligning the individual frames during reconstruction helped to improve the redundancy along time. Exploiting this enhanced sparsity during the CS reconstruction lead to an improved image quality. This observation is in accordance with previous work [9,19,20] where respiratory motion-compensated reconstruction also showed a positive effect on the resulting image quality. At the same time, visual inspection of the data showed no artificially introduced geometric deformation of the heart that may be introduced by the non-rigid registration. This is ensured by utilizing a diffeomorphic image registration providing inverse-consistent motion fields that were then used for motion-correction. In addition, the motion-compensation was only applied during the regularization term, while the data fidelity term constantly compared the reconstructed image to the actually acquired data.

While automated quantitative and qualitative perfusion assessment algorithms are on the research horizon and may prove to serve as a more objective assessment tool in the future [21,22], today clinical perfusion assessment is mostly based on visual image assessment. In both sequences all patients with ischemic lesions on coronary angiography, also had identifiable perfusion defects. While this is true on the patient level, which is clinically most important as any positive non-invasive stress testing may trigger an angiography, there were difference between SPARSE and TurboFLASH on segment level with regard to the extent of an ischemic lesion. When compared to reference standard, 98 % of true-positive ischemic segment were detected using SPARSE,

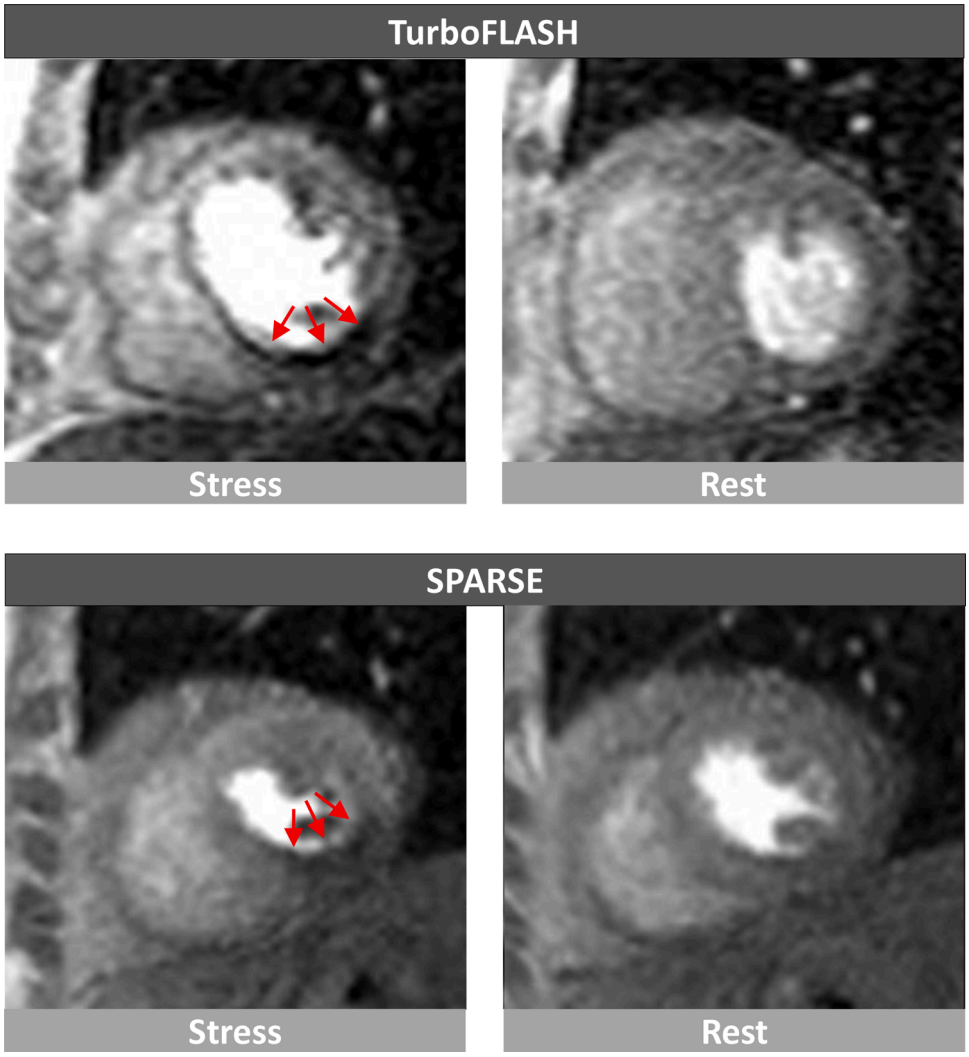

Fig. 3. Illustrative examples for perfusion defects with TurboFLASH and SPARSE sequence. White arrows indicate regions of ischemia.

Table 4
Diagnostic accuracy. Cross-table showing number of patients with true/false positive/negative perfusion readings for each sequence.

	TurboFLASH	SPARSE
True positive	19	19
False positive	3	1
False negative	0	0
True negative	1	3

TurboFLASH revealed 95 % of ischemic segments correctly. There is a possibility that this relatively small difference between the sequences may be attributable to different slice positions due to alternating breathing pattern or minimal difference in slice planning, however, image quality analysis suggests that higher CNR and fewer artifacts may favor SPARSE for more reliable ischemia detection.

In addition to qualitative assessment of ischemia, we also quantitatively compared the extent of perfusion defects using two different evaluation methods – upslope MPR and Fermi deconvolution analysis. Both methods consistently showed no difference in MPR between TurboFLASH and SPARSE, which is in line with results from other working groups using different CS perfusion sequences [17,23].

CS techniques can enable an increased, if not full, myocardial wall coverage on stress perfusion imaging. This may further enhance diagnostic accuracy for relevant CAD since even smaller ischemic lesions may become detectable. Other groups have shown hints for additional accuracy benefits for whole heart coverage using 3D perfusion sequences [24,25]. Large clinical trials such as MR-INFORM [26] have demonstrated that stress perfusion imaging even in three short axis myocardial planes is non-inferior to invasive FFR measurements with respect to detection of prognostically relevant myocardial ischemia. However, decreased spatio-temporal resolution and high variability of results remain obstacles to overcome [27]. In the present study sequence parameters for SPARSE and TurboFLASH were chosen similarly to allow for comparison. Future studies are necessary to evaluate additional benefits of increased myocardial coverage and further increased spatio-temporal resolutions with SPARSE and other CS perfusion techniques.

4.1. Conclusion

CS perfusion sequences such as SPARSE are non-inferior to conventional perfusion sequences with regard to diagnostic performance of myocardial stress perfusion MR imaging. They may add additional benefit by overcoming the current spatiotemporal resolution limit while providing sufficient myocardial CNR and reducing subendocardial dark-rim artifacts.

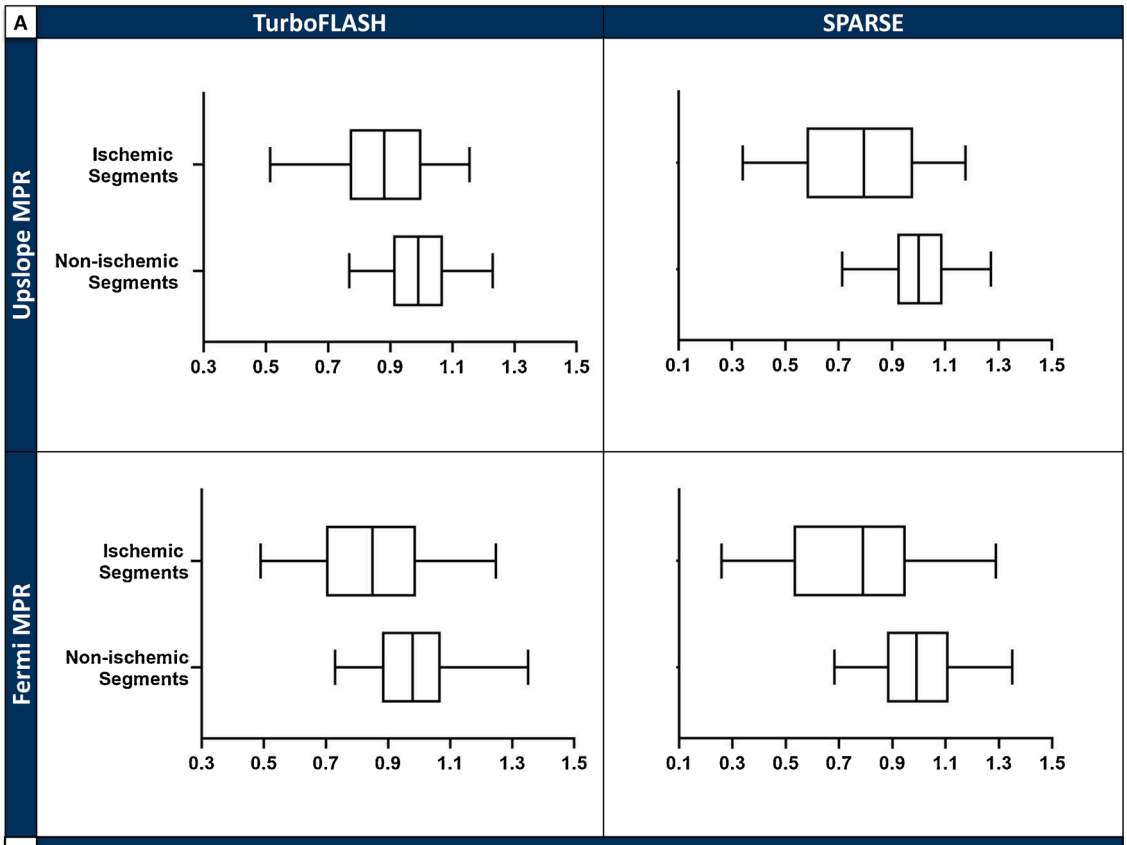

B

	Sequence	Non-ischemic segments	Ischemic segments	p value (Non-ischemic vs. ischemic)	p value (TurboFLASH vs. SPARSE)
Upslope MPR	TurboFLASH	1.00 ± 0.01	0.87 ± 0.01	<0.001	0.06
	SPARSE	1.00 ± 0.02	0.78 ± 0.02	<0.001	
Fermi MPR	TurboFLASH	1.00 ± 0.01	0.84 ± 0.02	<0.001	0.13
	SPARSE	1.00 ± 0.02	0.76 ± 0.03	<0.001	

Fig. 4. Quantitative perfusion analysis. Non-ischemic and ischemic segments refer to reference standard (FFR). MPR = myocardial perfusion reserve; FFR = fractional flow reserve.

4.2. Limitations

This trial was performed in a single-center setup with one single 1.5T MR system. The time interval between the two cardiac MR exams was relatively long due to healthcare system-related approval delays. Sequence parameters were not equal between both tested sequences (i.e. voxel size and image reconstruction method) which may significantly affect SNR and CNR comparability. Quantification of perfusion was only performed in a semi-quantitative fashion since we did not apply the dual-bolus technique.

Ethics approval and consent to participate

The study was approved local ethics board. Reference number: EA1/081/15

Consent for publication

Individuals have given their written consent for anonymous publication.

Consent for study participation

Study individuals have given their written consent for participating in this study.

Availability of data and materials

The datasets analyzed during the current study are available from the corresponding author upon reasonable request. Original imaging data are not publicly available due to lawful data protection in Germany.

Funding

This research did not receive any specific grant from funding agencies in the public, commercial, or not-for-profit sectors.

CRediT authorship contribution statement

FM developed study design (conceptualization, methodology), applied for ethic board approval, conducted major part of CMR scans

(investigation), led formal image analysis and data interpretation and was the major contributor in writing the manuscript (writing original draft and review editing, visualization).

AS conducted parts of CMR scans and major parts of the image analysis and statistical data interpretation (investigation, formal analysis).

CF was involved in image reconstruction, formal analysis and manuscript writing.

MS was involved in image reconstruction, formal analysis and manuscript review.

LR was involved in image reconstruction and formal analysis

MD was involved in data interpretation and manuscript review (writing original draft).

RG was involved in image reconstruction, analysis and manuscript review (writing original draft).

CS was involved in statistical analysis and manuscript review (writing original draft).

JS supervised overall study design, ensured quality control on image analysis and data interpretation, supervised manuscript writing and provided continuous guidance throughout study realization as head of the working group.

All authors have read and approved the final manuscript.

Declaration of Competing Interest

The authors report no declarations of interest.

Appendix A. Supplementary data

Supplementary material related to this article can be found, in the online version, at doi:https://doi.org/10.1016/j.ejrad.2020.109213.

References

[1] A.R. Patel, P.F. Antkowiak, K.R. Nandalur, et al., Assessment of advanced coronary artery disease: advantages of quantitative cardiac magnetic resonance perfusion analysis, J. Am. Coll. Cardiol. 56 (7) (2010) 561–569.

[2] M.J. Lipinski, C.M. McVey, J.S. Berger, C.M. Kramer, M. Salerno, Prognostic value of stress cardiac magnetic resonance imaging in patients with known or suspected coronary artery disease: a systematic review and meta-analysis, J. Am. Coll. Cardiol. 62 (9) (2013) 826–838.

[3] C.M. Kramer, J. Barkhausen, S.D. Flamm, R.J. Kim, E. Nagel, Society for Cardiovascular Magnetic Resonance Board of Trustees Task Force on standardized P, Standardized cardiovascular magnetic resonance (CMR) protocols 2013 update, J. Cardiovasc. Magn. Reson. 15 (2013) 91.

[4] J.P. Greenwood, N. Maredia, J.F. Younger, et al., Cardiovascular magnetic resonance and single-photon emission computed tomography for diagnosis of coronary heart disease (CE-MARC): a prospective trial, Lancet 379 (9814) (2012) 453–460.

[5] S. Plein, S. Ryf, J. Schwitter, A. Radjenovic, P. Boesiger, S. Kozerke, Dynamic contrast-enhanced myocardial perfusion MRI accelerated with K-t sense, Magn. Reson. Med. 58 (4) (2007) 777–785.

[6] J. Tsao, P. Boesiger, K.P. Pruessmann, k-t BLAST and k-t SENSE: dynamic MRI with high frame rate exploiting spatiotemporal correlations, Magn. Reson. Med. 50 (5) (2003) 1031–1042.

[7] M. Lustig, D. Donoho, J.M. Pauly, Sparse MRI: the application of compressed sensing for rapid MR imaging, Magn. Reson. Med. 58 (6) (2007) 1182–1195.

[8] G. Morton, M. Ishida, A. Schuster, et al., Perfusion cardiovascular magnetic resonance: comparison of an advanced, high-resolution and a standard sequence, J. Cardiovasc. Magn. Reson. 14 (1) (2012) 34.

[9] E. Nagel, C. Klein, I. Paetsch, et al., Magnetic resonance perfusion measurements for the noninvasive detection of coronary artery disease, Circulation 108 (4) (2003) 432–437.

[10] H. Yoon, K.S. Kim, D. Kim, Y. Bresler, J.C. Ye, Motion adaptive patch-based low-rank approach for compressed sensing cardiac cine MRI, IEEE Trans. Med. Imaging 33 (11) (2014) 2069–2085.

[11] S.G. Lingala, E. DiBella, M. Jacob, Deformation corrected compressed sensing (DC-CS): a novel framework for accelerated dynamic MRI, IEEE Trans. Med. Imaging 34 (1) (2015) 72–85.

[12] B.B. Avants, C.L. Epstein, M. Grossman, J.C. Gee, Symmetric diffeomorphic image registration with cross-correlation: evaluating automated labeling of elderly and neurodegenerative brain, Med. Image Anal. 12 (1) (2008) 26–41.

[13] P. Montesinos, J.F. Abascal, L. Cusso, J.J. Vaquero, M. Desco, Application of the compressed sensing technique to self-gated cardiac cine sequences in small animals, Magn. Reson. Med. 72 (2) (2014) 369–380.

[14] T. Wech, W. Pickl, J. Tran-Gia, C. Ritter, M. Beer, D. Hahn, H. Kostler, Whole-heart cine MRI in a single breath-hold–a compressed sensing accelerated 3D acquisition technique for assessment of cardiac function, RoFo 186 (1) (2014) 37–41.

[15] B. Sharif, R. Arsanjani, R. Dharmakumar, C.N. Bairey Merz, D.S. Berman, D. Li, All-systolic non-ECG-gated myocardial perfusion MRI: feasibility of multi-slice continuous first-pass imaging, Magn. Reson. Med. 74 (6) (2015) 1661–1674.

[16] G. Adluru, C. McGann, P. Speier, E.G. Kholmovski, A. Shaaban, E.V. Dibella, Acquisition and reconstruction of undersampled radial data for myocardial perfusion magnetic resonance imaging, J. Magn. Reson. Imaging 29 (2) (2009) 466–473.

[17] N. Maredia, A. Radjenovic, S. Kozerke, A. Larghat, J.P. Greenwood, S. Plein, Effect of improving spatial or temporal resolution on image quality and quantitative perfusion assessment with k-t SENSE acceleration in first-pass CMR myocardial perfusion imaging, Magn. Reson. Med. 64 (6) (2010) 1616–1624.

[18] M. Li, T. Zhou, L.F. Yang, Z.H. Peng, J. Ding, G. Sun, Diagnostic accuracy of myocardial magnetic resonance perfusion to diagnose ischemic stenosis with fractional flow reserve as reference: systematic review and meta-analysis, JACC Cardiovasc. Imaging 7 (11) (2014) 1098–1105.

[19] R. Zhou, W. Huang, Y. Yang, et al., Simple motion correction strategy reduces respiratory-induced motion artifacts for k-t accelerated and compressed-sensing cardiovascular magnetic resonance perfusion imaging, J. Cardiovasc. Magn. Reson. 20 (1) (2018) 6.

[20] M. Usman, D. Atkinson, F. Odille, Motion corrected compressed sensing for free-breathing dynamic cardiac MRI, Magn. Reson. Med. 70 (2) (2013) 504–516.

[21] L.Y. Hsu, M. Jacobs, M. Benovoy, et al., Diagnostic performance of fully automated pixel-wise quantitative myocardial perfusion imaging by cardiovascular magnetic resonance, JACC Cardiovasc. Imaging 11 (5) (2018) 697–707.

[22] J. Betancur, Y. Otaki, M. Motwani, et al., Prognostic value of combined clinical and myocardial perfusion imaging data using machine learning, JACC Cardiovasc. Imaging 11 (7) (2018) 1000–1009.

[23] N.K. Naresh, X. Chen, R.J. Roy, P.F. Antkowiak, B.H. Annex, F.H. Epstein, Accelerated dual-contrast first-pass perfusion MRI of the mouse heart: development and application to diet-induced obese mice, Magn. Reson. Med. 73 (3) (2015) 1237–1245.

[24] R. Manka, L. Wissmann, R. Gebker, et al., Multicenter evaluation of dynamic three-dimensional magnetic resonance myocardial perfusion imaging for the detection of coronary artery disease defined by fractional flow reserve, Circ. Cardiovasc. Imaging 8 (5) (2015).

[25] R. Manka, C. Jahnke, S. Kozerke, et al., Dynamic 3-dimensional stress cardiac magnetic resonance perfusion imaging: detection of coronary artery disease and volumetry of myocardial hypoenhancement before and after coronary stenting, J. Am. Coll. Cardiol. 57 (4) (2011) 437–444.

[26] E. Nagel, J.P. Greenwood, G. McCann, et al., Magnetic resonance perfusion or fractional flow reserve in coronary disease, N. Engl. J. Med. 380 (25) (2019) 2418–2428.

[27] L. Wissmann, A. Gotschy, C. Santelli, et al., Analysis of spatiotemporal fidelity in quantitative 3D first-pass perfusion cardiovascular magnetic resonance, J. Cardiovasc. Magn. Reson. 19 (1) (2017) 11.